Journal of Catalysis **207,** 183–193 (2002)
doi:10.1006/jcat.2002.3522, available online at http://www.idealibrary.com on IDEAL®

Cycloisomerization of 5-(o-Tolyl)-Pentene over Modified Zeolite BEA

Dae Hyun Choo,* Hae Jin Kim,† Byung Hee Kong,§ Il Seok Choi,§ Young Chan Ko,§ Hee Cheon Lee,† Jae Chang Kim,‡ and Jae Sung Lee[1,*]

*Department of Chemical Engineering/School of Environmental Science and Engineering, and †Department of Chemistry/Division of Molecular and Life Science, Pohang University of Science and Technology (POSTECH), San 31 Hyoja-dong, Pohang 790-784, Korea; ‡Department of Chemical Engineering, Kyungpook National University, Taegu 702-701, Korea; and §S-Oil Corporation, R&D Center, 360 Sanam-ri, Onsan-eup, Ulju-kun, Ulsan, 689-890, Korea

Received May 29, 2001; revised January 9, 2002; accepted January 9, 2002

Liquid-phase cycloisomerization of 5-(o-tolyl)-pentene (OTP) was conducted using a commercial nanocrystalline zeolite BEA. Zeolite BEA was a good catalyst for selective synthesis of 1,5-dimethyltetralin (1,5-DMT). However, over certain zeolite BEA, isomerization of 1,5-DMT to other isomers occurred after cyclization of OTP was almost complete at high temperatures. Textual properties of nanocrystalline BEA did not influence the cyclization activity, but the degree of postsynthetic treatments such as surface poisoning, passivation, and dealumination had great effects. Reactions over BEA modified by triphenylphosphine poisoning and Si layer coating of the outer surface of zeolite crystallites revealed that strong acid sites residing only on the external surface of zeolite BEA were responsible for isomerization activity. The ^{27}Al magic-angle spinning nuclear magnetic resonance study for dealuminated zeolites together with the IR study of adsorbed pyridine clearly demonstrated that the concentration of Brønsted acid sites due to the framework aluminum was directly related to cyclization activity. On the other hand, octahedral aluminum did not participate in either OTP cyclization or DMT isomerization. © 2002 Elsevier Science (USA)

Key Words: **1,5-dimethyltetralin; zeolite BEA; passivation; ^{27}Al NMR; Brønsted acid sites; microcrystallites; surface poisoning; external surface acidity.**

INTRODUCTION

1,5-Dimethyltetralin (1,5-DMT) is a useful intermediate for synthesizing 2,6-naphthalenedicarboxylic acid (2,6-NDCA), a raw material used to make polyethylene naphthalate (PEN). 1,5-DMT can be obtained from 5-(o-tolyl)-pent-1-ene (i), 5-(o-tolyl)-pent-2-ene (ii), and their mixture (hereafter referred to as OTP) through cyclization over acidic zeolite catalysts (Fig. 1). After cyclization, 1,5-DMT (iii) undergoes dehydrogenation to produce 1,5-dimethylnaphthalene (1,5-DMN), isomerization to produce 2,6-DMN, and finally oxidation to 2,6-NDCA (1).

[1] To whom correspondence should be addressed. Fax: 82-54-279-5799. E-mail: jlee@postech.ac.kr.

When OTP is cyclized with conventional zeolite catalysts, side reactions accompany the cyclization due to further isomerization and dehydroisomerzation of 1,5-DMT. Due to these side reactions involving isomerization, less-useful DMT (iv) and DMN isomers are produced in significant amounts. Because of their similar physical properties, DMT and DMN isomers are difficult to separate to give the pure 1,5-isomer. Further, it is known that these by-products, once converted to DMNs, are virtually impossible to isomerize completely into a desired isomer, for isomerization of DMNs occurs within the same triad in the isomers of naphthalene rings (within 1,5-, 1,6-, and 2,6-isomers; 1,3-, 1,4-, and 2,3-isomers; 1,7-, 1,8-, and 2,7-isomers, respectively), according to Fries' law.

Many patents disclosed techniques for preparing 1,5-DMT from OTP with various modified zeolite catalysts, such as Pd- and Pt-impregnated Y (1), USY, and BEA (2–6). Though BEA is known to have the highest activity among these catalysts, side products of isomerization remain the key problem in obtaining 1,5-DMT selectively.

There is no report concerned directly with the low selectivity problem in OTP cyclization over zeolite BEA. Some research groups, however, have reported that acid sites on the external surface of the zeolite crystals may affect selectivity for fine chemical synthesis (7, 8). Thus, we cannot ignore the effect caused by the outer surface of microcrystalline BEA having relatively high external surface areas (over 200 m^2/g vs ca. 700 m^2/g of total area).

According to van Bekkum and coworkers (9) and Prins and coworkers (10), the acid sites on the external surface of the zeolite crystals influence reaction by their own strong acidity or by deposition of cokelike materials near the pore mouth resulting in the problem of reactant accessibility. In order to remove external surface acidity, they introduced bulky materials such as tetraethylorthosilicate (TEOS) as a source of Si layer passivation and triphenylphosphine as a surface-poisoning reagent. By applying the passivated BEA samples to several reactions, they showed that TEOS treatment of BEA effectively removed external surface

0021-9517/02 $35.00

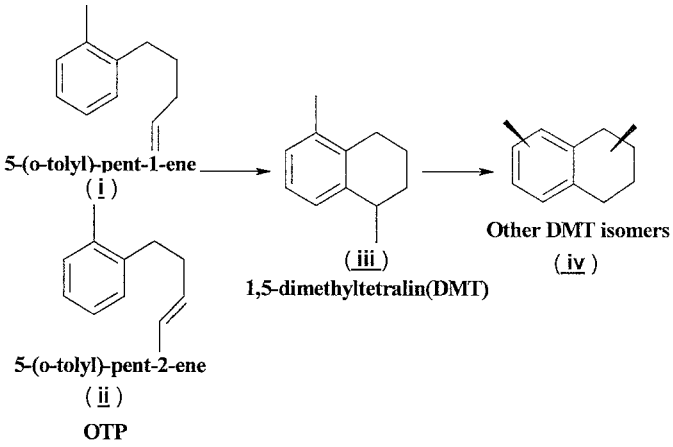

FIG. 1. A reaction scheme of cycloisomerization of OTP over zeolite BEA.

acidity permanently and the Si layer remained even after repetitive regenerations. Furthermore, through catalytic activity tests over BEA using various crystal sizes, they reported that the activity of catalysts with relatively large crystal sizes was more effectively controlled by passivation of external surface due to the ease of Si layer formation and its stability after calcination (9, 10).

In the present work, we investigate the effect of external surface acidity in OTP cycloisomerization using modified commercially prepared nanocrystalline BEA and look for any relationship between structural difference and reactivity. In addition, we show how framework Al concentration affects cyclization activity by studying dealuminated BEA using ^{27}Al magic-angle spinning (MAS) nuclear magnetic resonance (NMR) and adsorbed pyridine using Fourier transform infrared (FT-IR).

EXPERIMENTAL

Materials and Postsynthetic Modifications

Through passivation and dealumination treatments, samples of zeolite BEA with various Si/Al ratios and different external surface acidity were obtained and tested for cycloisomerization of OTP.

Commercial BEA samples were purchased from Tosoh Co., Japan (denoted BEA1) and PQ Co., U.S.A. (BEA2). They were in the NH_4^+ form when purchased. All the samples were calcined to obtain the H-form at 773 K for 4 h in air (75 μmol s^{-1}) before reaction.

Chemical liquid deposition was performed to passivate the external surface of the zeolites (9). Tetraethylorthosilicate (TEOS; Aldrich, 99%+) was used as Si source. TEOS (0.2 g/g of catalyst) was stirred under nitrogen atmosphere for 2 h. After deposition, obtained samples were stirred and filtered with *n*-hexane (Aldrich 99%) to remove residual TEOS. Finally the samples were calcined for 4 h with air at 773 K before reaction.

The dealumination of BEA was carried out using nitric acid of various concentrations (30 ml/g of catalyst) at 353 K for 4 h under reflux condition. To remove residual acid and impurities, samples were repeatedly washed and filtered. After dealumination, samples were dried for 24 h in an oven at 383 K and calcined for 4 h at 773 K in air (75 μmol s^{-1}) before reaction.

In designation of various BEA samples, the letter "P" identifies passivated samples. Dealuminated samples are denoted by "D" followed by the concentration of acid used for the treatment. For example, BEA1-D-1 denotes a dealuminated BEA1 sample (from Tosoh Co.) treated with 1 N nitric acid and BEA2-P is a passivated BEA2 (from PQ Co.) sample.

Characterization

The quantitative analysis of Si, Al, and mineral impurities was performed by means of atomic absorption spectroscopy (AAS) on a Perkin–Elmer AAS 5100PC. The surface Si/Al ratio was calculated from the X-ray photoelectron spectroscopy (XPS) peak areas of Si 2p and Al 2p obtained on a Perkin–Elmer Phi5400 ESCA (Mg $K\alpha$, 350 W). Nitrogen adsorption isotherms were obtained at 77 K using a Micrometrics ASAP 2010C sorption apparatus. Cold-field emission scanning electron micrographs (FE-SEM) were recorded on a Hitachi S-4200 FE-SEM.

^{27}Al MAS NMR spectra were collected using a Varian Unity *Inova* 300 spectrometer (7.4 T), equipped with a 7.5-mm Chemagnetics MAS probe. Magic-angle spinning (MAS) was carried out at a rotor speed of 5.5 kHz and $Al(H_2O)_6^{3+}$ was referenced to 0 ppm. The ^{27}Al MAS NMR spectra were recorded with a pulse sequence of a single $\pi/2$ pulse (2.5 μs), 400–1000 accumulated scans, and a recycle-delay time of 0.1 s. Dehydrated samples for ^{27}Al MAS NMR were prepared on a modified shallow-bed Cavern apparatus (12). The sample was heated to 773 K (1 K/min), evacuated at 773 K for 12 h under a 10^{-5} Torr vacuum, and then transferred to a 7.5-mm zirconia MAS rotor after cooling to room temperature.

The FT-IR spectroscopy of adsorbed pyridine was used to analyze acid properties of zeolite BEA. A self-supported wafer (ca. 10 mg/cm^2) was placed in an infrared cell made of quartz with a CaF_2 window, heated to 773 K at a rate of 5 K/min under vacuum (5×10^{-5} Torr), and evacuated for 2 h. On cooling to 473 K, pyridine (Aldrich, 99.8%, anhydrous) was adsorbed for 30 min and the sample was evacuated at 523 K for 2 h. Following this pretreatment, IR spectra in the 1400- to 1700-cm^{-1} region were recorded using a Perkin–Elmer 1800.

Catalytic Activity Measurements

All the chemicals were purchased from Aldrich Chemical Co. and stored in the presence of zeolite 13X before

reaction. Bulk 2,6-DMN (95%+) was kindly provided by S-Oil Corporation.

As a standard for gas chromatograph analysis, 1,5-DMT was synthesized from hydrogenation of 1,5-DMN as follows: 1 g of 1,5-DMN (Aldrich, 98%) and 3 g of isopentyl alcohol (99%+, anhydrous) were stirred at 413 K for 5 h with metallic Na (lump in kerosene, 99%). After reaction, alkoxide was extracted with deionized water, and residual alcohol and water were removed by distillation. 2,6-DMT and 2,7-DMT were prepared in the same ways. The obtained DMT mixture contained small quantities of dimethyldihydronaphthalene and dimethyltrihydronaphthalene impurities that were identified with gas chromatography/masspectrometry (GC/MS).

A liquid-phase cycloisomerization reaction was carried out in a sealed batch reactor under nitrogen equipped with a magnetic stirrer. Reactions were carried out in the temperature range 373–518 K under nitrogen pressure with 0.5–3 wt% catalyst/OTP.

Catalytic activity of triphenylphosphine-poisoned BEA was measured under the same condition mentioned above. Before reaction, triphenylphosphine (1 or 5 wt% catalyst samples) was added to the catalyst dissolved in the *n*-tetradecane as solvent and stirred for 0.5 h at room temperature.

The reaction products were analyzed quantitatively by gas chromatography on a Hewlett Packard 5890 series II equipped with a HP PONA 50-m capillary column and were identified by GC/MS (HP 5890 IIGC/597 MS Detector) analysis.

RESULTS

Reaction Conditions for Cycloisomerization

Product distribution. As can be seen in Fig. 2, all BEA samples maintained high selectivity in the cyclization of OTP. Only BEA1, however, showed activity for isomerization to other DMTs. Contrary to DMN isomerization known to occur within a triad position of the naphthalene ring (1), 1,5-DMT was converted to isomers belonging to other triads (2,7-DMT and 1,7-DMT) in addition to the one within the same triad (2,6-DMT).

Most interesting, in the case of BEA2, we could see only cyclization activity and the rate of OTP conversion was substantially slower than for BEA1. While BEA1 showed a characteristic concentration-time curve typical for a series reaction, BEA2 did not. We attempted isomerization of 1,5-DMT as reactant over BEA2 and obtained only trace amounts of other DMT isomers. This result implies that the poor activity of BEA2 for DMT isomerization cannot be explained by the slow formation of the intermediate (1,5-DMT) but by the absence of the isomerization activity on BEA2.

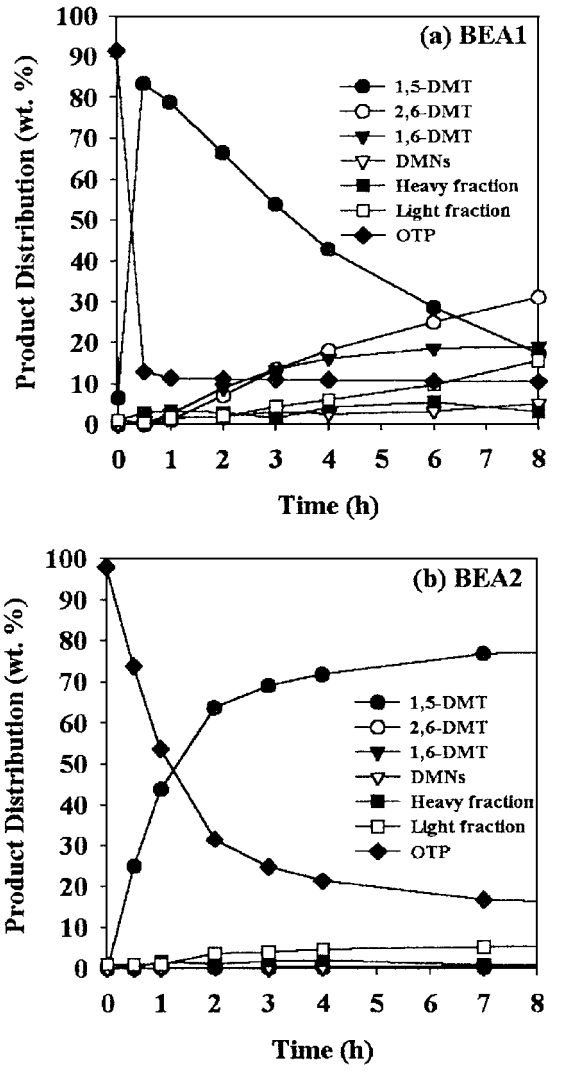

FIG. 2. Product distribution of OTP cycloisomerization over (a) zeolite BEA1 and (b) BEA2 (1 wt% catalyst/OTP, 473 K).

Effect of catalyst weight and temperature. With BEA1, the dependence of 1,5-DMT selectivity on catalyst weight and reaction temperature was investigated and the results are shown in Figs. 3 and 4, respectively.

As can be seen in Fig. 3, more than 95% of OTP was converted to 1,5-DMT in 0.5 h regardless of catalyst (BEA1) loading. In the case of the 8-h reaction, however, the high selectivity for 1,5-DMT was maintained only with the 0.5 wt% catalyst loading, and the selectivity abruptly decreased with increasing catalyst loadings. The temperature effect of the reaction was investigated in Fig. 4 for 2 wt% BEA1/OTP in the temperature range 373–474 K. 1,5-DMT was obtained selectively at low temperatures but isomerization to other DMT isomers was observed above 443 K. These results clearly show that some acid sites exist on BEA1 that are responsible for the isomerization of DMT, and the reaction occurs only at higher temperatures. The rate of DMT

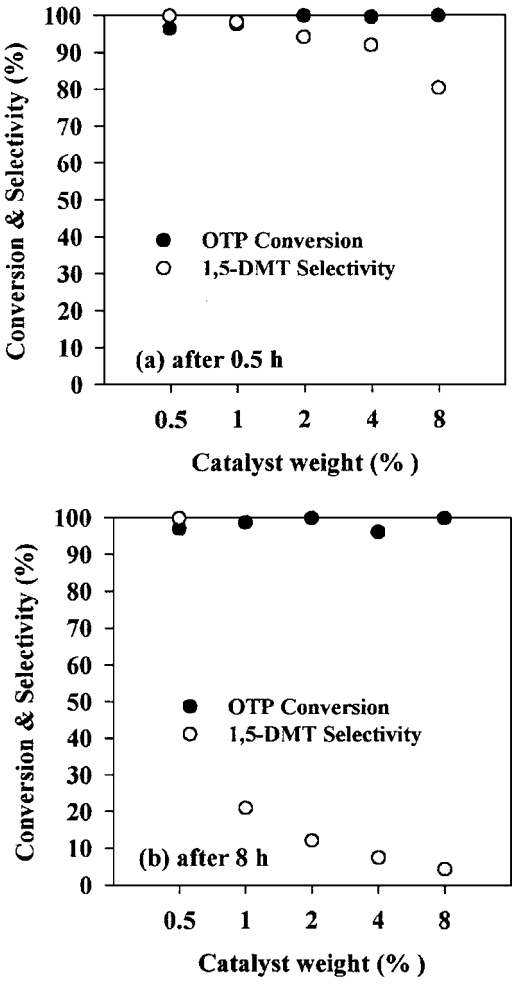

FIG. 3. OTP conversion and 1,5-DMT selectivity versus catalyst weight over BEA1 (473 K) after a (a) 0.5-h and (b) 8-h reaction.

isomerization, however, seems much slower than that of OTP cyclization, and high 1,5-DMT selectivities could be obtained only at short reaction times, small catalyst loadings, and low reaction temperatures.

BEA2 showed the same trend of change in OTP conversions with increasing catalyst weights and temperatures, yet isomerization to other DMTs was not observed even at high temperatures and with high catalyst loadings (13). Furthermore, BEA2 showed relatively lower activity in cyclization of OTP throughout all conditions, as shown in Fig. 2b. Thus, there must be a difference in properties between the two BEA zeolite catalysts that play more important roles than do reaction conditions in the cycloisomerization of OTP.

Comparison of BEA Samples by FE-SEM and N_2 Adsorption

The SEM images are shown in Fig. 5. BEA1 samples consisted of aggregates with diameters of 0.5–1 μm that were made of spherical primary crystallites, whereas aggregates of BEA2 samples had diameters less than 150 nm. Primary crystallites of both BEA1 and BEA2 samples were smaller than 50 nm and could be called "microcrystallites" or "nanocrystallites." Based on the SEM images, we could expect that all samples would have high external surface areas.

The physical properties derived from N_2 adsorption/desorption data are summarized in Table 1 together with Si/Al ratios determined by chemical analysis. High external surface areas (ESAs) obtained from the slope of the *t*-plot of the N_2 isotherm are consistent with the presumption based on FE-SEM images (13). Also, the shape of N_2 isotherms of calcined BEA1 and BEA2 was in accordance with that reported for nanocrystalline BEA of high Al content prepared by Camblor *et al.* (14).

BET areas of passivated samples decreased slightly, suggesting that the coated Si layer effectively smoothed the rough outer surface. The ESA of BEA1 was reduced

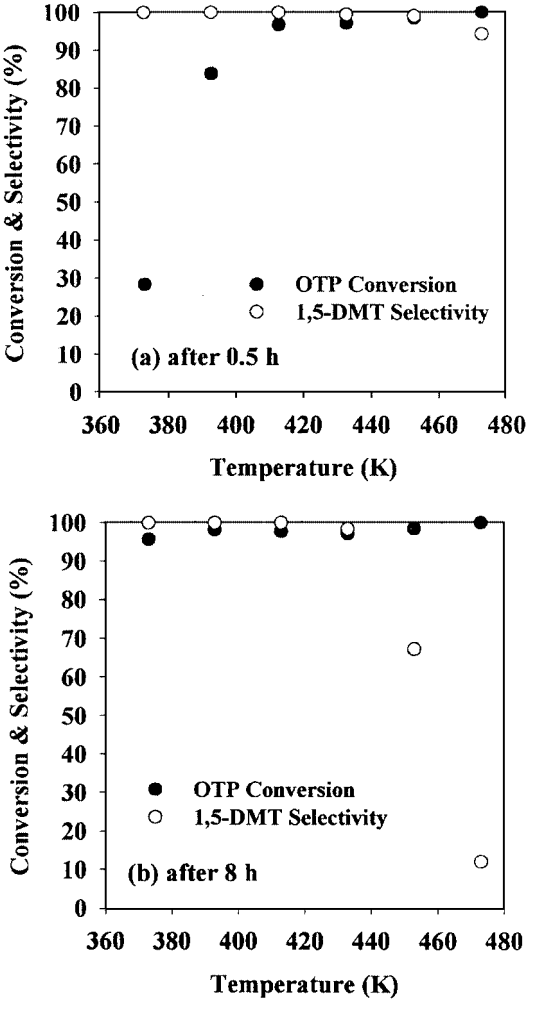

FIG. 4. OTP conversion and 1,5-DMT selectivity versus reaction temperature over BEA1 (2 wt% catalyst/OTP) after a (a) 0.5-h and (b) 8-h reaction.

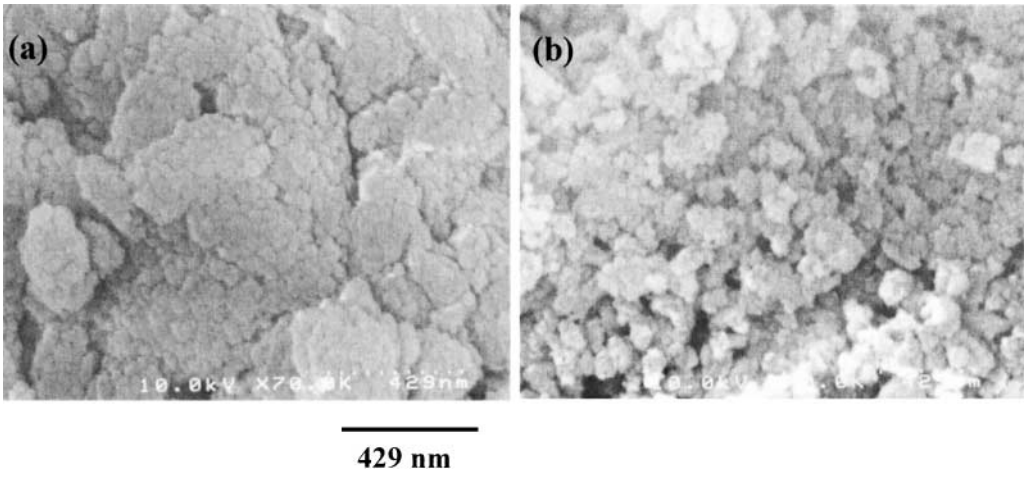

FIG. 5. FE-SEM images of (a) BEA1 and (b) BEA 2.

more markedly, because interparticle volumes of aggregates, which would be interpreted as ESA in N_2 adsorption measurements, were filled up with several-nanometer-thick Si layers. However, ESA of BEA2 was not reduced much due to its relatively small degree of aggregation. Almost constant micropore volumes for both BEA samples indicate that the passivation treatment may not affect their inner pore system.

External Surface Poisoning with Triphenylphosphine

To eliminate external surface activity, the cyclization of OTP was carried out with triphenylphosphine-poisoned catalysts (1 or 5 wt%). Because triphenylphosphine has too large a size to enter inner pores of zeolite BEA, it can be used to eliminate selectively external surface acidity of zeolite crystals (7) by adsorption on the external Brønsted acid sites (15).

From ^{31}P MAS NMR (not shown), we observed that triphenylphosphine adsorbed on the external surface without significant decomposition and with only small amounts of triphenylphosphine converted to other unidentified phosphine species.

Figure 6 shows the effects of triphenylphosphine addition on conversion and 1,5-DMT selectivities of BEA catalysts. The conversions to 1,5-DMT decreased with an increasing amount of triphenylphosphine. The selectivities were high for all cases and did not change significantly with triphenylphosphine loading. Triphenylphosphine is known to deactivate preferentially external surface Brønsted acid sites and block gradually the pore mouth as its amount is increased. In the case of BEA1 treated with 1 wt% triphenylphosphine, incomplete poisoning of the inner part of aggregates caused negligible reduction in conversion but eliminated isomerization reactivity completely. However, even with the small amount of triphenylphosphine, the

TABLE 1

Physical Properties of BEA Samples

Sample	Si/Al		Crystallinity[c] (%)	BET area (m^2/g)	Micropore volume (cm^3/g)	External surface area (m^2/g)	Micropore area (m^2/g)
	Bulk[a]	Surface[b]					
BEA1	14	13.8	81	625	0.16	282	343
BEA1-D-0.5	20	15.4	82	679	0.18	299	379
BEA1-D-1	21	—	78	698	0.19	297	401
BEA1-D-10	42	—	69	742	0.20	311	430
BEA2	17	11.6	110	605	0.17	240	365
BEA2-D-0.5	73	—	106	629	0.18	246	383
BEA2-D-1	81	—	106	635	0.18	248	386
BEA2-D-10	126	—	102	661	0.19	254	407
BEA1-P	16	—	—	579	0.16	236	343
BEA2-P	18	—	—	563	0.16	221	342

[a] By chemical analysis.
[b] By XPS.
[c] Determined from intensities of an X-ray diffraction peak $2\theta = 22.5^\circ$ relative to those for the ammonium form of BEA1 and BEA2.

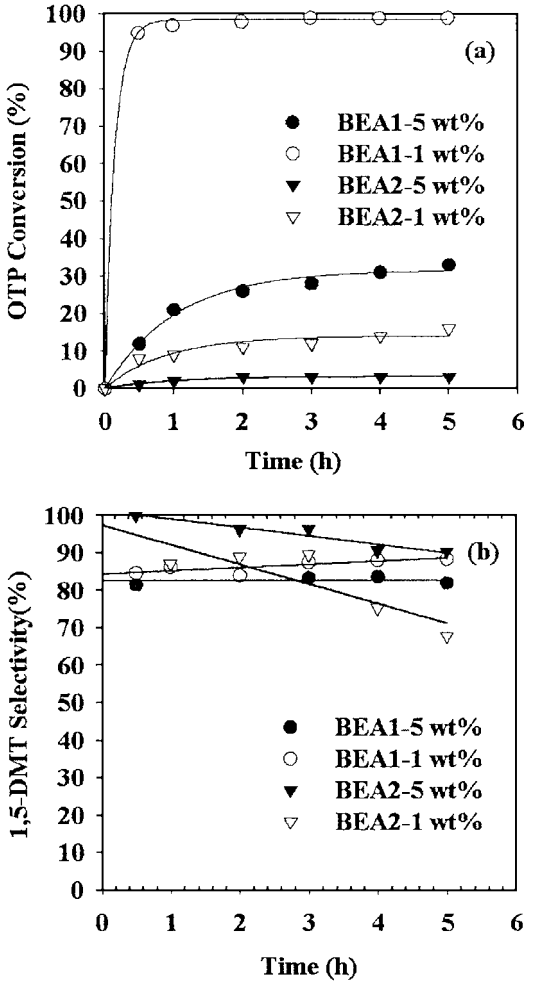

FIG. 6. Conversion (a) and selectivity (b) of OTP cycloisomerization (2 wt% catalyst/OTP, 473 K) over poisoned BEA (1 and 5 wt% triphenylphosphine/catalyst).

poisoning effect was much more serious for BEA2. BEA2 has a relatively short internal pore length and its internal sites also appear to be affected by triphenylphosphine poisoning.

These results imply that only external surface acidity is related to DMT isomerization and that morphology of BEA aggregates may affect the extent of poisoning by triphenylphosphine.

Passivation of External Surface with TEOS

The external surface acidity was removed by silica coating with TEOS for BEA1 and BEA2. The effect of this surface passivation with TEOS on OTP cycloisomerization is shown in Fig. 7. BEA1-P showed almost the same activity of OTP cyclization and complete suppression of DMT isomerization activity. BEA2-P exhibited only 70% of the activity of calcined BEA2 before passivation and no activity for DMT isomerization even after a 7-h reaction.

These results demonstrate that the formed silica layer effectively passivates the external surface acid sites without significant effects on sites inside the pores. According to Kunkeler *et al.* (9), passivation treatment can be more effectively applied to the macrocrystalline BEA, for microcrystalline BEA has a rough external surface which could interfere with the formation of Si layer and cause the destruction of the Si layer during calcination. In our cases, however, passivation treatment successfully removed external surface acidity although both BEA1 and BEA2 are microcrystalline crystals.

From these facts, we might consider that OTP cyclization and DMT isomerization take place at different acid sites. Together with the poisoning experiment with triphenylphosphine, it can be proposed that 1,5-DMT isomerization occurs only at the external Brønsted acid sites while OTP cyclization is mainly related to acid sites of the inner channel.

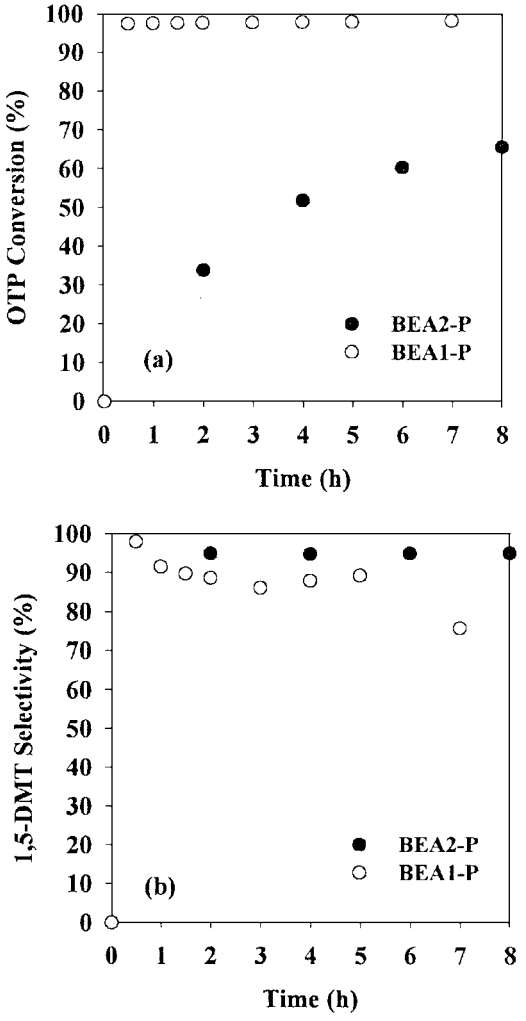

FIG. 7. Conversion (a) and selectivity (b) of OTP cycloisomerization (2 wt% catalyst/OTP, 473 K) over passivated BEA (0.2 g of TEOS/g of catalyst).

Effect of Dealumination

As discussed above, it appeared that only external surface acidity affected 1,5-DMT isomerization. Yet, the low OTP cyclization activity for BEA2 could not be explained by structural difference and/or external surface acidity. Thus, to investigate further the relationship between the nature of acid sites and OTP cyclization activity, we tested dealuminated BEA zeolites for the reaction.

As shown in Fig. 8, dealuminated BEA2 showed a reduced activity in OTP cyclization. BEA2-D-0.5 showed about 20% reduction in OTP cyclization activity compared with the untreated BEA2, but no reactivity for isomerization of DMT. The severe dealumination treatment with 10 N nitric acid (BEA2-D-10) induced complete deactivation for both cyclization and isomerization. Dealuminated BEA1 maintained high activity for OTP cyclization but did not show DMT isomerization activity at all, and it appeared that acid treatment removed external surface acidity. There was not much difference in activity and selectivity among dealuminated BEA1 treated with nitric acid of different concentrations.

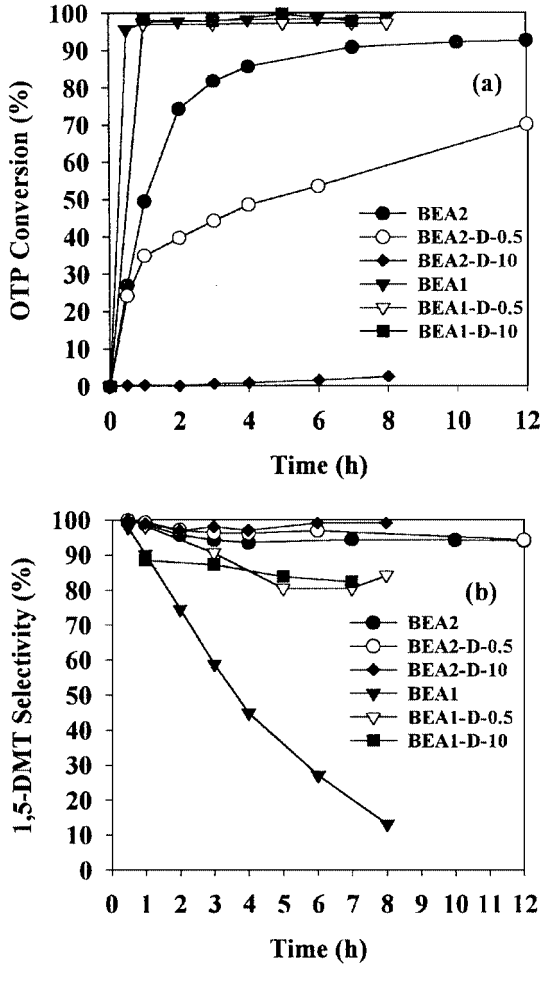

FIG. 8. Conversion (a) and selectivity (b) of OTP cycloisomerization over dealuminated BEA (1 wt% catalyst/OTP, 473 K).

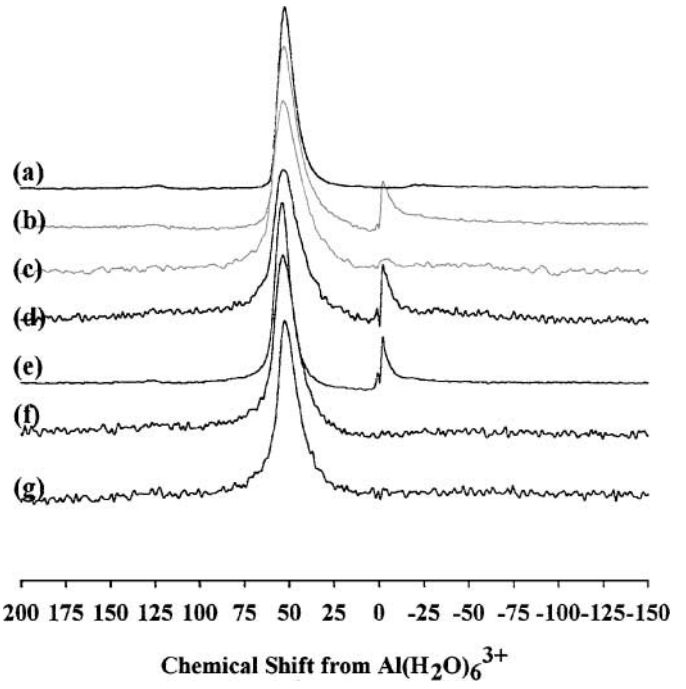

FIG. 9. ^{27}Al MAS NMR spectra of dealuminated BEA1: (a) NH_4^+ form, (b) BEA1, (c) dehydrated BEA1, (d) BEA1-P, (e) BEA1-D-0.5, (f) BEA1-D-1, and (g) BEA1-D-10.

Dealuminated samples showed reduced activity for OTP cyclization. However, BEA1 samples had consistently higher activity than BEA2 irrespective of Si/Al ratios. Thus, BEA1-D-10 with a relatively high Si/Al ratio had a higher activity than untreated BEA2. There must be some other factor that is responsible for the different activities of the two BEA zeolites from different sources.

^{27}Al MAS NMR and FT-IR Studies

Figures 9 and 10 show ^{27}Al MAS NMR spectra of modified BEA1 and BEA2 samples, respectively.

According to Jansen *et al.* (16), Brønsted acid sites are located on both external and internal surfaces and Lewis sites are on the internal defect sites. Furthermore, the environment of Al atoms is known to be related to two acid sites: Lewis acid sites due to octahedrally connected Al (Oh-Al) and Brønsted acid sites attributed to tetrahedrally coordinated framework Al (Td-Al). From ^{27}Al multiple-quantum (MQ) MAS study, Müller *et al.* (17) assigned a peak at 60 ppm as tetrahedrally coordinated framework Al, a peak at 0 ppm as octahedrally coordinated "extraframework" Al, and a peak between 30 and 50 ppm as penta-coordinated Al and/or distorted tetrahedrally coordinated extraframework Al. On the other hand, Fajula and coworkers (18) and van Bekkum and coworkers (19) noted that Oh-Al was partially connected

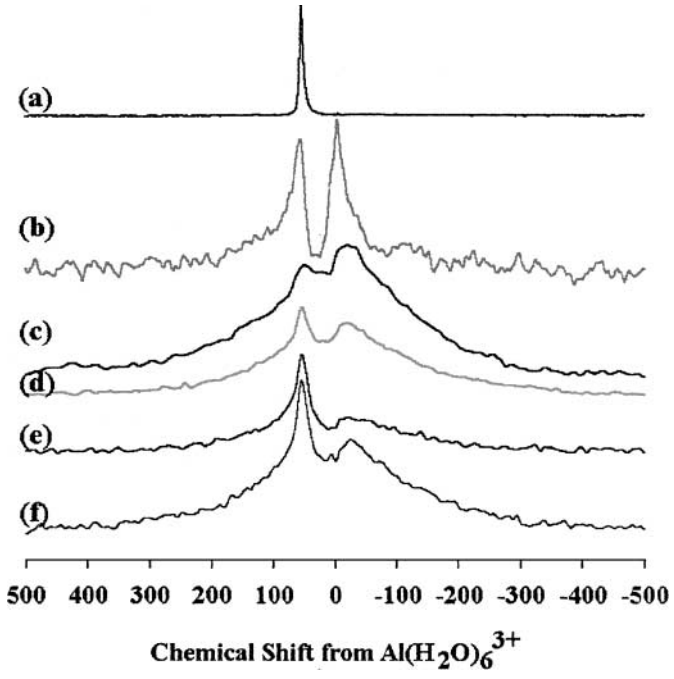

FIG. 10. ^{27}Al MAS NMR spectra of dealuminated BEA2: (a) NH_4^+ form, (b) BEA2, (c) dehydrated BEA2, (d) BEA2-D-0.5, (e) BEA2-D-1, and (f) BEA2-D-10.

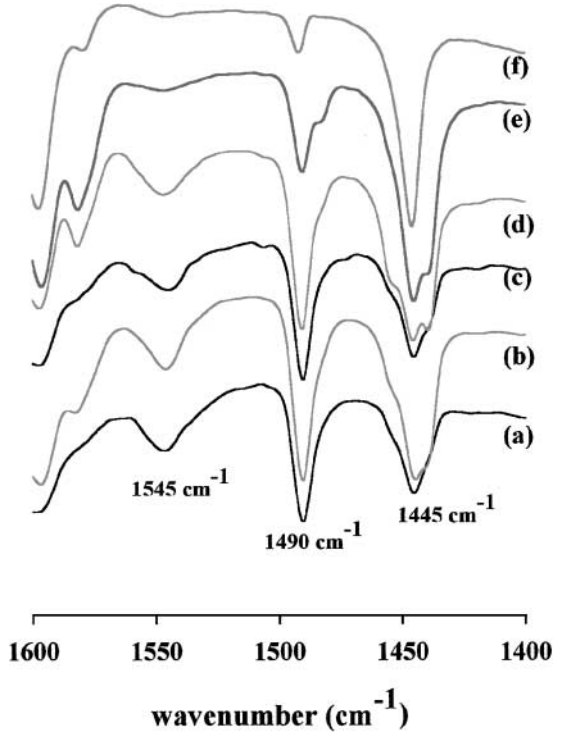

FIG. 11. Infrared spectra of pyridine-adsorbed dealuminated BEA: (a) BEA1, (b) BEA1-D-0.5, (c) BEA1-D-10, (d) BEA2, (e) BEA2-D-05, and (f) BEA2-D-10.

framework Al through tetrahedral–octahedral interconversions.

In Fig. 9, tetrahedrally coordinated framework Al at 54 ppm and octahedrally coordinated Al at 0 ppm appeared for calcined and slightly dealuminated BEA1 samples (BEA1-D-0.5), but the Oh-Al peak disappeared as dealumination progressed to a higher extent. This is in a good agreement with what Bourgeat-Lami *et al.* reported (20). The Oh-Al peak was also observed in BEA1-P. We could not distinguish two Td-Al sites that were reported to exist, due to two different crystallographic sites of BEA (21) near 54 ppm. However, we observed two Si(0Al) sites in separate ^{29}Si MAS spectra (22).

Contrary to BEA1, the ^{27}Al MAS NMR spectra of BEA2 samples shown in Fig. 10 have much broadened linewidths, indicating that considerable amounts of randomly distributed Al species are present. We pretreated all the samples with so-called "deep bed calcination" (16), and BEA2 showed an intense Oh-Al peak and broad peaks superimposed between 0 and 50 ppm due to Al species with a low symmetry.

As the concentration of nitric acid used for dealumination treatment increased, the Oh-Al peak intensities of BEA2 gradually decreased and their linewidths became much broader. However, unlike the case with BEA1, the Oh-Al peak appeared even for the sample treated with 10 N nitric acid. Dealuminated BEA1 samples also showed broadened Td-Al peaks, although the degree of broadening was insignificant compared with those of the BEA2 samples.

Infrared spectra recorded on pyridine adsorption on dealuminated BEA are presented in Fig. 11. With the exception of dealuminated BEA2 (Figs. 11e and 11f), three typical peaks appeared in the range 1400–1600 cm^{-1} due to vibrations of adsorbed pyridine over BEA zeolites. IR bands at 1545 and 1445 cm^{-1} correspond to pyridinium ion adsorbed on Brønsted acid sites and pyridine on Lewis acid sites, respectively. The band at 1490 cm^{-1} is caused by pyridine adsorbed on both Brønsted and Lewis acid sites. All BEA1 samples showed a strong IR band at 1545 cm^{-1} and this band still remained for dealuminated BEA1. However, only traces of this peak were detected for dealuminated BEA2.

DISCUSSION

Several postsynthetic treatments were conducted to obtain a suitable catalyst for selective formation of 1,5-DMT while suppressing the formation of other isomers. Among the isomers obtained from 1,5-DMT isomerization, 2,6-DMT could be converted to 2,6-DMN directly and is a desirable product. Some investigators have tried to make 2,6-DMN from commercially less-useful other DMN + DMT isomers, especially the 2,7-triad, by hydroisomerization/dehydrogenation with a noble metal/acidic

silica–alumina catalyst (23). In 1,5-DMT isomerization over zeolite BEA1, we also obtained 2,6-DMT as the main product. However, small amounts of 2,7-triad isomers still remained (included in light fraction, Fig. 2). In our previous study (13), reactions with zeolites of different pore systems, Y and mordenite, showed similar product distribution. From these facts, we might consider that isomerization of 1,5-DMT to 2,6-DMT is not subject to any shape selectivity.

In any case, selective synthesis of 1,5-DMT without further isomerization to other triad isomers is more desired in this stage of the 2,6-NDCA manufacturing process. For this purpose, BEA1 modified by surface passivation or dealumination should be the catalyst of choice. Untreated BEA2 is also selective for 1,5-DMT synthesis, but the reaction rates are low.

Results of several postsynthetic modifications of BEA zeolites revealed that only external surface acidity was responsible for the isomerization of once-formed 1,5-DMT to other DMT isomers. The sites were present only on the outer surface of zeolite particles and removed completely by triphenylphosphine adsorption or surface passivation by the Si layers. Ideally, surface poisoning or passivation would not affect either textual or acidic properties of inner pore system. Furthermore, isomerization of 1,5-DMT as reactant over BEA1-P with relatively high activity for cyclization of OTP showed no conversion to other DMT isomers. These results imply that the isomerization activity observed over BEA1 is not due to any process occurring inside the zeolite pores, including the internal diffusion limitation. From the ^{27}Al NMR spectra shown in Fig. 9, BEA1-P showed a similar framework Si/Al ratio to that of untreated BEA1, yet negligible isomerization activity. Thus, acid density cannot explain isomerization activity either. Interpretation of the reactivity of dealuminated catalysts is more complicated, because the dealumination treatment would modify the pore structure. However, the high selectivity for these catalysts could also be explained by the expulsion of isomerization sites by the dealumination treatment. We were not able to identify the external acid sites responsible for isomerization directly with any spectroscopic characterization tools. They might be present in a small concentration. However, their presence is evident from the reactivities of these modified zeolites. The most interesting is the difference between two BEA zeolites procured from different sources. BEA2 does not show any isomerization activity even without poisoning or passivation of its outer surface. Also, as mentioned, it shows much lower activity in OTP cyclization.

From FE-SEM and N_2 adsorption/desorption isotherm data, we observed a definite difference in bulk structure between BEA1 and BEA2. In spite of similar external surface areas, BEA1 is aggregated on a larger scale compared to BEA2. However, these textual differences between two BEA zeolites could not account for such a great difference in OTP cycloisomerization activity. Although BEA1 is in the form of large aggregates, its higher activity indicates that there is no hindrance of reactant access to the interparticle volume. Thus, different textual properties between BEA1 and BEA2 are significant, but they are insufficient to explain the differences in the activity and selectivity of these catalysts in OTP-to-DMT reactions.

In contrast, the degree of dealumination for nitric acid-treated samples clearly shows the effect of these textual differences (see Table 1). Thus, BEA1 was only slightly dealuminated with strong acid treatments, whereas BEA2 was easily dealuminated with even weaker acid treatments. The Si/Al ratio of BEA1-D-10 was 42 and that of BEA2-D-0.5 was 73. The different effect of acid treatments can be understood in terms of the difference in the degree of aggregation that affects contact between nitric acid and framework Al atoms. Additionally, the existence of an amorphous moiety or unstable structures in original BEA2 can be an alternative explanation. The slight increase in crystallinity after acid treatment and the higher fraction of nonframework Al species observed by ^{27}Al NMR supports the possibility.

Catalytic activity measurements for dealuminated samples show the relationship between framework Al and OTP conversion. As the bulk Si/Al ratio measured by elemental analysis increased, the conversion to 1,5-DMT decreased rapidly for the dealuminated BEA2 samples. However, calcined BEA1 and BEA2 with similar bulk Si/Al ratios (14 and 17, respectively) showed a large difference in activity in OTP cyclization; BEA1 showed higher activity even in a more dealuminated state. Then, which property of BEA zeolites is responsible for the different activity in OTP cyclization? We calculated the framework Al concentration from the intensity of the peak at 54 ppm in ^{27}Al MAS NMR spectra. Figure 12 shows a relationship between this

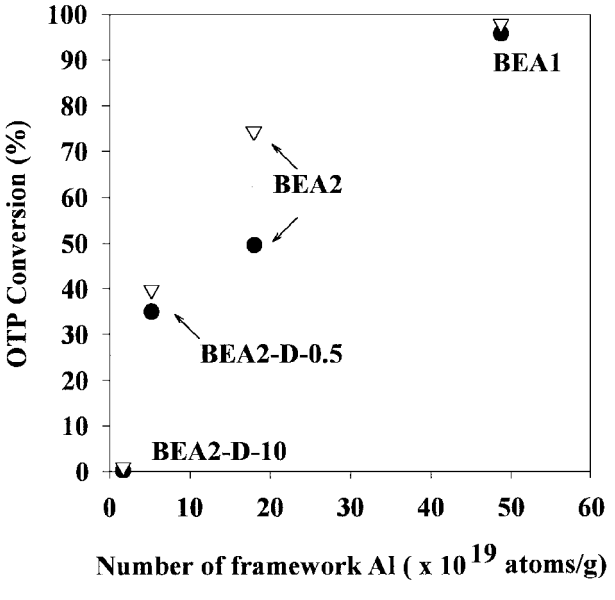

FIG. 12. A correlation between framework Al concentrations of BEA and OTP conversions after 1-h (●) and 2-h (▽) reaction (1 wt% catalyst/OTP, 473 K).

number of framework Al and OTP conversion after a 1- and 2-h reaction. The correlation is good. As Al atoms lose their symmetry by acid dealumination or steaming, the number of extraframework Al and/or unsaturated framework Al increases, and some portions of Al sites cannot be observed with simple ^{27}Al MAS NMR due to the existence of so-called "invisible Al" (17). Furthermore, dehydration/rehydration treatments and residual water significantly influence the spectral shape, and consequently, the interpretation of ^{27}Al NMR spectrum is complicated (18, 24).

To examine any disappearance or chemical shift of peaks due to water, ^{27}Al MAS NMR were also conducted for BEA1 and BEA2 further dehydrated by treating calcined samples at 773 K (Figs. 9c and 10c, respectively). Though dehydrated BEA1 (Fig. 9c) exhibited reduced intensity of the Oh-Al site, the overall lineshape did not change. The ^{27}Al MAS NMR spectrum of dehydrated BEA2 still showed a broad and intense peak at 0 ppm after treatment and the spectrum is similar to that of dehydrated BEA reported by Deng *et al.* (24). The similar spectral shape of BEA1 and dehydrated BEA1 implies that the relatively narrow linewidth of BEA1 samples is not the effect of moisture or calcination methods but of different Al environments between BEA1 and BEA2. The difference in the NMR peak intensity of the same sample due to dehydration did not exceed 10%. Hence, the good correlation between the intensity of Td-Al NMR peaks and activity in OTP cyclization might be interpreted as Brønsted acid sites due to this Td-Al being responsible for the activity in OTP cyclization.

Infrared spectra of pyridine adsorbed on zeolites (Fig. 11) clearly support the relationship between framework Al concentration and Brønsted acid sites. The intensity of the IR band at 1545 cm^{-1} assigned to pyridinium ions rapidly decreases for dealuminated BEA2 (Figs. 12e and 12f). However, that of dealuminated BEA1 still remains without a significant change in band intensity. The IR band at 1445 cm^{-1}, which corresponds to pyridine bonded to a Lewis acid site, shows little changes for all the samples, and therefore, the ratio of Brønsted acid/Lewis acid concentration is higher for BEA1 and dealuminated BEA1. Brønsted acid sites of zeolites are responsible for the IR band of pyridinium ions and consequently its strong band intensity means that BEA1 have a lot of tetrahedrally coordinated Al.

The ^{27}Al MAS NMR spectra of BEA1, BEA1-D-0.5 and BEA1-P, and all BEA2 samples showed an Oh-Al peak at 0 ppm. Whereas only BEA1 showed activity for DMT isomerization, the high activity for OTP cyclization was maintained for three BEA1 samples showing the Oh-Al peak. Thus, there was no correlation between the Oh-Al peak and activity and selectivity of OTP reactions. From these facts, it might be concluded that Oh-Al is related to neither OTP cyclization nor DMT isomerization. More detailed discussions about the nature of Oh-Al species through NMR characterization is the subject of a forthcoming publication (22).

CONCLUSIONS

We have investigated selective cyclization of OTP over BEA zeolites obtained from different sources and subjected to different postsynthetic modifications. The major side reaction, the isomerization of once-formed 1,5-DMT to other DMT isomers, followed OTP cyclization as a typical series reaction. The sites responsible for the isomerization appear to be strong acid sites residing on the external surface of the zeolite crystal and are effectively removed by triphenylphosphine poisoning, Si layer coating, or dealumination. The activity of OTP cyclization showed a good correlation with the amount of framework aluminum measured by ^{27}Al MAS NMR. These results together with FT-IR of adsorbed pyridine indicate that the Brønsted acid sites are responsible for the OTP cyclization activity. On the other hand, octahedral Al species did not participate in either OTP cyclization or DMT isomerization.

ACKNOWLEDGMENT

This work was supported by the Brain Korea 21 project and the S-Oil Co.

REFERENCES

1. Sikkenga, D. L., Zaenger, I. C., and Williams, G. S., U.S. Patent 5,118,892 (1992).
2. Sikkenga, D. L., Lamb, J. D., Zaenger, I. C., and Williams, G. S., U.S. Patent 4,950,825 (1990).
3. Sikkenga, D. L., Zaenger, I. C., and Williams, G. S., U.S. Patent 5,012,024 (1991).
4. Sikkenga, D. L., Zaenger, I. C., and Williams, G. S., U.S. Patent 5,030,781 (1991).
5. Sikkenga, D. L., Lamb, J. D., Zaenger, I. C., and Williams, G. S., U.S. Patent 5,073,670 (1991).
6. Sikkenga, D. L., Lamb, J. D., Zaenger, I. C., and Williams, G. S., U.S. Patent 5,401,892 (1995).
7. Creyghton, E. J., Elings, J. A., Downing, R. S., Sheldon, R. A., and van Bekkum, H., *Microporous Mater.* **5**, 299 (1996).
8. Harvey, G., Binder, G., and Prins, R., *Stud. Surf. Sci. Catal.* **94**, 397 (1995).
9. Kunkeler, P. J., Moeskops, D., and van Bekkum, H., *Microporous Mater.* **11**, 313 (1997).
10. Vogt, A., Kouwenhoven, H. W., and Prins, R., *Appl. Catal.* **123**, 37 (1995).
11. Andy, P., Garcia-Martinez, J., Lee, G., Gonzalez, H., Jones, C. W., and Davis, M. E., *J. Catal.* **192**, 215 (2000).
12. Bell, A. T., and Pines, A., *in* "NMR Techniques in Catalysis," p. 144. Dekker, New York, 1994.
13. Choo, D. H., M.S. thesis. Pohang University of Science and Technology, 1999.
14. Camblor, M. A., Corma, A., and Valencia, S., *Microporous Mesoporous Mater.* **25**, 59 (1998).

15. Balttusis, L., Frye, J. S., and Mariel, C. E., *J. Am. Chem. Soc.* **109**, 40 (1987).
16. Jansen, J. C., Creyghton, E. J., Njo, S. L., Henk van Koningsveld, H., and van Bekkum, H., *Catal. Today* **38**, 205 (1997).
17. Müller, M., Harvey, G., and Prins, R., *Microporous Mesoporous Mater.* **34**, 281 (2000).
18. De Ménorval, L. C., Buckermann, W., Figueras, F., and Fajula, F., *J. Phys. Chem.* **100**, 465 (1996).
19. Kunkeler, P. J., Zuurdeeg, B. J., van der Waal, J. C., van Bokhoven, J. A., Koningsberger, D. C., and van Bekkum, H., *J. Catal.* **180**, 234 (1998).
20. Bourgeat-Lami, E., Massiani, P., Di Renzo, F., Espiau, P., Fajula, F., and Des Couriéres, T., *Appl. Catal.* **72**, 139 (1991).
21. Zaiku, X., Qingling, C., Chengfang, Z., Jiaqing, B., and Yuhua, C., *J. Phys. Chem. B* **104**, 2853 (2000).
22. Choo, D. H., Kim, H. J., and Lee, J. S., manuscript in preparation.
23. Santilli, D. S., and Chen, C. Y., U.S. Patent 6,015,930 (2000).
24. Deng, F., Yue, Y., and Ye, C., *J. Phys. Chem.* **102**, 5252 (1998).